GROWTH MORPHOLOGIES OF QUASICRYSTALLINE PHASE IN A BULK UNDERCOOLED AFMr (Si, B) ALLOY

Song Guangsheng, Yang Gencang and Zhou Yaohe
State Key Lab of Solidification Processing,
Northwestern Polytechnical University, Xi' an 710072, P. R. China

ABSTRACT The complex method of glass covering, salt denucleating and multiple superheating cooling has been successfully applied to undercool the melt of a bulk AFMn (Si, B) alloy and initiate quasicrystalline phase at an undercooling of 100 K. Growth morphologies of the quasicrystalline phase were characterized by using scanning electron microscopy (SEM) and transmission electron microscopy (TEM). SEM and TEM imagies indicate 5-fold and 3-fold symmetric faceting dendrites, and dendrite elements and polyhedron particles, respectively. The constitution level and relation to m3 5 point group symmetry of growth morphology for the undercooled quasicrystalline phase have been reported for the first time.

Key words AFM m (Si, B) high undercooling quasicrystalline phase growth morphology

1 INTRODUCTION

In 1984, Shechtman et al^[1] firstly reported that they had found the icosahedral quasicrystalline phase in an AFM n alloy. From then on, the rapidly quenched AFTM (TM = transition metals) alloys have been widely studied. The additions of non transition metals have been proved to be able to improve the microstructure and stability of the icosahedral phase in rapidly quenched AFM mX alloys such as AFM mSi^[2] and AFM mB^[3] alloys. The icosahedral quasicrystalline phase has m3 5 point group symmetry and fast 5-fold and 3-fold growth directions^[4, 5].

Limited by heat conduction, only low-dimensional quasicrystalline alloys can be produced by rapid quenching, while the thermodynamic undercooling caused by melt purification is not limited by volume in principle, the high undercooling rapid solidification can be used to produce bulk quasicrystalline alloys. Chen $et\ al^{[6]}$ prepared a $d6\ \mathrm{mm}$ single icosahedral phase ball of Al65Cu20Fe15 alloy through multiple superheating cooling purification of the alloy in a

quartz tube heated by a high frequency induction heater, and studied the solidification mechanism and formation ability of the icosahedral phase under high undercooling conditions. Herlach et al^[7] obtained a bulk Al58Cu34Fe8 alloy of d7 mm by containerless electromagnetic levitation method and studied the preferred nucleation mechanism of the icosahedral phase. However, no reports can be found about the relation of the new growth morphology of the highly undercooled icosahedral phase and its m3 5 point group symmetry.

The authors of this paper adopted the complex method of glass covering, salt denucleating and multiple superheating-cooling method to deal with an AFM n binary alloy, prepared a bulk AFM m(Si, B) icosahedral alloy by high undercooling, and placed the emphasis on the relation of the new growth morphology of the undercooled icosahedral phase and its m3 5 point group symmetry.

2 EXPERIMENTAL

The master alloy was prepared by induction

① Project 59671045 supported by the National Natural Science Foundation of China and project 96G53081 supported by the Aeronautical Science Foundation of China Received Jul. 24, 1997; accepted Nov. 10, 1997

melting of 99. 999% Al and 99. 7% Mn covered with B₂O₃ particles in a quartz tube in air. The mixture of the master alloy and the specially made salt was contained in a quartz tube to be remelted and purified by using the multiple superheating cooling method, then a $d15 \text{ mm} \times$ 70 mm sample was obtained. The composition analysis of the remelted and purified alloy was performed using a spectrophotometer with a precision of 0.005%. High-precision SCIT infrared radiation pyrometer was used to moniter the temperature change of specimens with time. The microstrcture and phase composition were characterized by TEM and SEM equipped with EDX. In addition, differential thermal analyzer (DTA) was adopted to determine the liquidus and transition temperature of the alloy (heating rate: 20 K/min).

3 RESULTS AND DISCUSSION

3. 1 Alloy composition and analysis

The chemical composition of the studied alloy is AF27.6M m-4.6Si-0.008B. It can be seen that Si and B are introduced by chemical reaction in the melting process, and that the ratio of Si/B is very large. The circumstances are caused by the following reactions among the aluminum alloy melt, the quartz tube and the covering argent:

$$4Al+ 3SiO_2 \longrightarrow 2Al_2O_3 + 3[Si]$$
 (1)

$$2Al+ B2O3 \longrightarrow Al2O3 + 2[B]$$
 (2)

$$4[B] + 3SiO_2 \longrightarrow 2B_2O_3 + 3[Si]$$
 (3)

After remelting and salt denucleating, the content of Si in the alloy will increase continuously through reaction (1), but the deoxidizing product Al₂O₃ will be effectively removed by the specially made salt, accordingly the melt is purified as expected, and a bulk AFM m (Si, B) alloy with bright surface is obtained. Therefore. through the alloying of the directly added elements Al and Mn and the indirectly added elements Si and B, the alloys of expected elements can be in situ prepared, but the contents of the elements cannot be controlled strictly yet, which is due to the fact that the contents of Si and B introduced by chemical reactions are related with the melting process.

3. 2 Outward appearance of bulk quasicrystalline alloy

Fig. 1 shows the outward appearance of a bulk AFM m (Si, B) quasicrystalline alloy prepared by high undercooling. The surface of the sample is bright and pollution free. Brittle fracture occurs about half length of the rod, and the angle between the fracture surface and the center line is about 32°. The sample rod is 15 mm in drameter and 70 mm in length, which is the largest reported at home and abroad [7, 8].





Fig. 1 Outward appearance of bulk Al-Mrr (Si, B) quasicrystalline alloy

3. 3 Growth morphologies of undercooled quasicrystalline phase

Fig. 2 shows the temperature vs time curve of AFM r (Si, B) alloy in the solidification pro-The differential temperature analysis (DTA) curve of this alloy is given in the left lower side of Fig. 2, and the T_L temperature can be determined from the DTA curve. The TEM diffraction pattern is also given in the right upper side of Fig. 2, which shows the existence of the quasicrystalline phase. Because there will never occur 5-fold rotational symmetric diffraction patterns in any single crystals, it is used as an important evidence to identify the quasicrystalline phase. It can be seen from Fig. 2 that there occurs undercooling in the melt below the liquidus temperature of the quasicrystalline phase ($T_{\rm L}$ = 1293 K), and there initiates nuclei at T_N = 1193 K. Therefore, the undercooling in the specimen is $\Delta T = T_L - T_N = 100 \text{ K}$.

Figs. 3(a) and (b) show the SEM micrographs of the growth morphologies of the

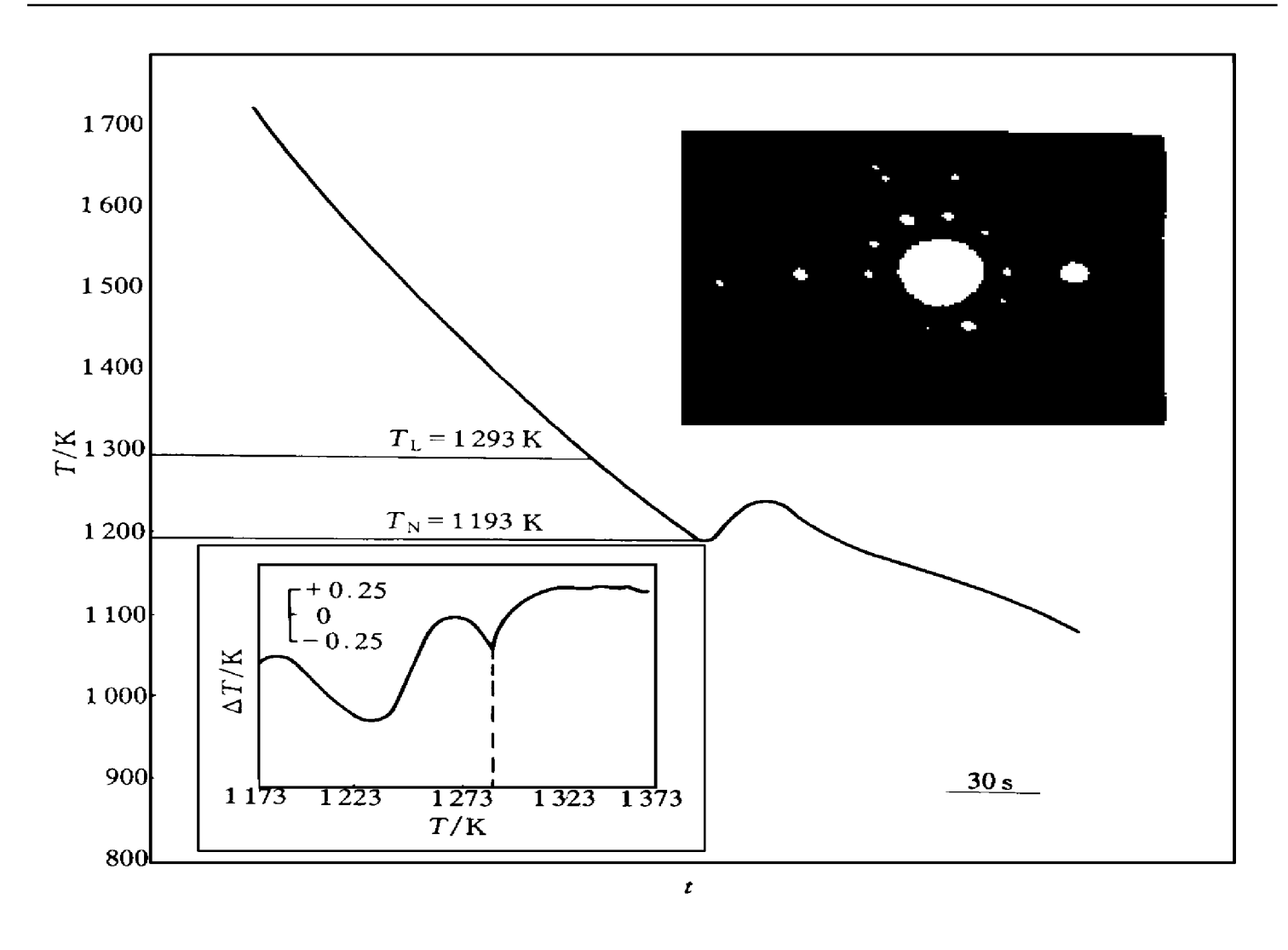


Fig. 2 Temperature vs time curve, TEM diffraction pattern and DTA curve of bulk Al-Mm (Si, B) quasicrystalline alloy

quasicrystalline phase. The quasicrystalline phase has been imbedded into the α -Al phase, which shows that the quasicrystalline phase first nucleates in the melt, and then the crystalline phase mucleates and grows.

Additionally, the quasicrystalline phase preferrably grows into symmetric dendrites and each dendrite is surrounded by facets, thus the quasicrystalline phase presents symmetric faceted dendritic morphology. EDX analysis indicates that the composition of the quasicrystalline phase is Al38M n6Si and no B element is detected because its content is below the lower limit of the measurement apparatus.

The quasicrystalline structure has 5-fold, 3-fold and 2-fold rotational symmetries, its point group symbol is m3 5, which does not belong to any of the 32 Bravis crystal point groups. A regular icosahedron has 12 vertexes, the link line of

each vertex and the center is a 5-fold rotational symmetric axis, and the angles between neighbouring link lines are 63.43°. If the fast growth directions are along the link lines, then star-like grains will be obtained. Different morphologies will be observed if a quasicrystalline grain is cut off along different highly symmetric axes. Fig. 3 (c) is a schematic diagram of a grain which grows in the link line directions, i. e. an elevational drawing observed along a 5-fold zone axis. This figure is the result of the overlapping of two 5-fold symmetric faceted dendrites. If a grain is cut perpendicular to a 5-fold zone axis at two sides of the grain center, one will see a 5-fold symmetric morphology as shown in Fig. 3(a). Fig. 3(d) is a schematic diagram of an elevational drawing observed along a 3-fold, which is the result of the overlapping of two 3-fold symmetric faceted dendrites. If a grain is cut perpendicular

to a 3-fold zone axis far from or near the grain center, then 3 or 6 dendritic arms will be observed respectively. Fig. 3(b) is a morphology of the latter case. Therefore, the growth morphologies of the undercooled quasicrystalline phase are 5-fold or 3-fold faceted dendrites, and have the same m3 5 point group symmetry as the quasicrystalline structure. These unique growth morphologies of the quasicrystalline phase can describe its specific characteristics and are also determined by the structure. Icosahedral grains of similar morphologies have been reported in Al17M n^[4] and Ti62Fe27M n8. 5Si2. 5 alloys. But there is an obvious difference between the morphologies of the two former alloys and those observed by the authors; for the two formers,

their 5-fold or 3-fold morphologies are five or three dendritic arms appropriately spaced around a vacant center, while for the undercooled AFM m (Si, B) alloy, its 5-fold or 3-fold morphologies are five or three faceted dendritic arms appropriately spaced around a solid center. This difference in morphology between the undercooled quasicrystalline phase and the rapidly quenched phase is caused by the differences of solidification conditions and compositions.

The substructures of the quasicrystalline phase can be further studied by high resolution TEM. Fig. 4 shows the bright field morphologies of the quasicrystalline phase. The low-magnification morphology in Fig. 4(a) shows that there are no obvious primary and secondary

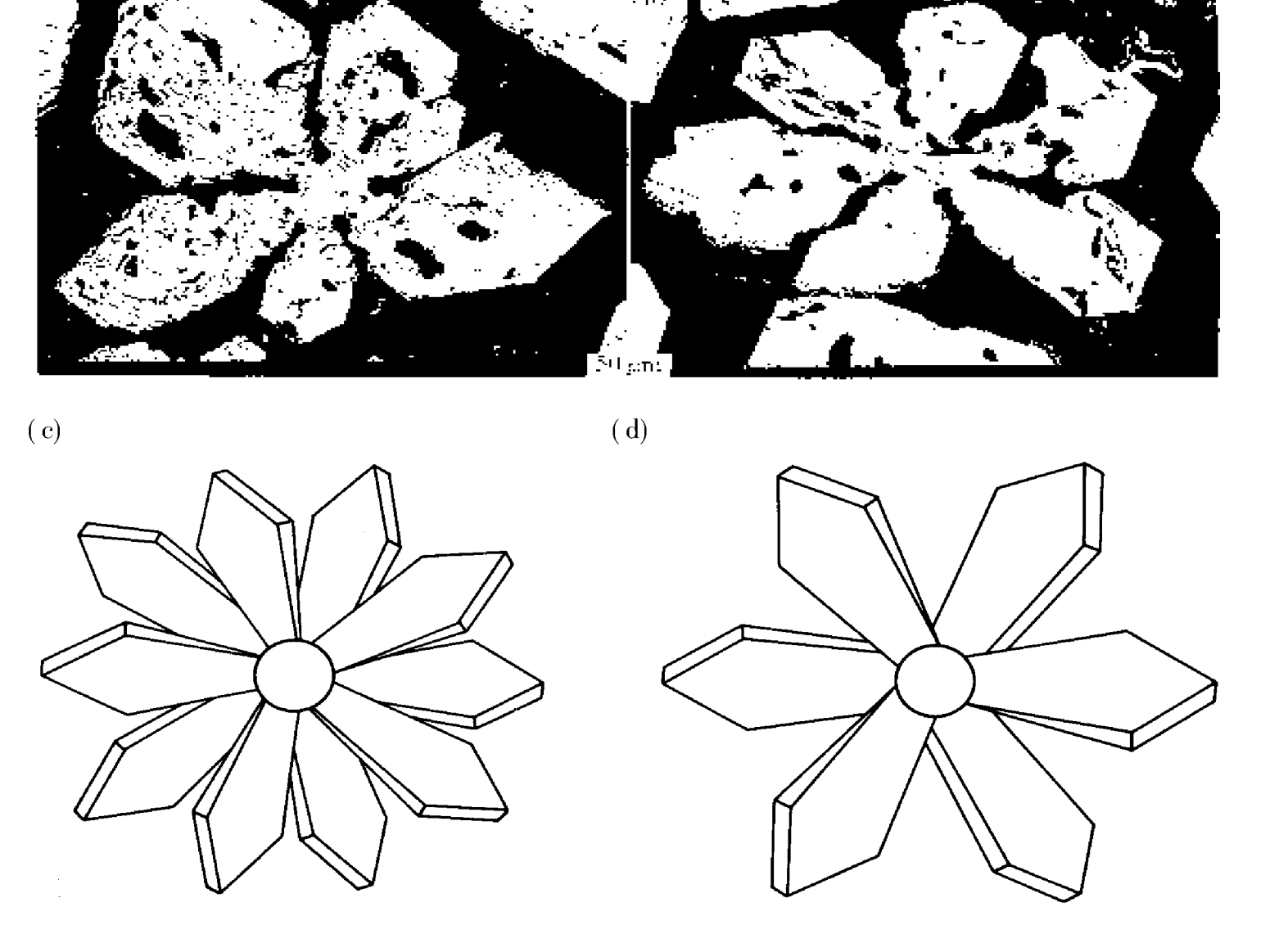


Fig. 3 SEM micrographs of quasicrystalline grains observed along 5-fold zone axis (a) and corresponding schematic (c) and along 3-fold zone axis (b) and corresponding schematic (d)

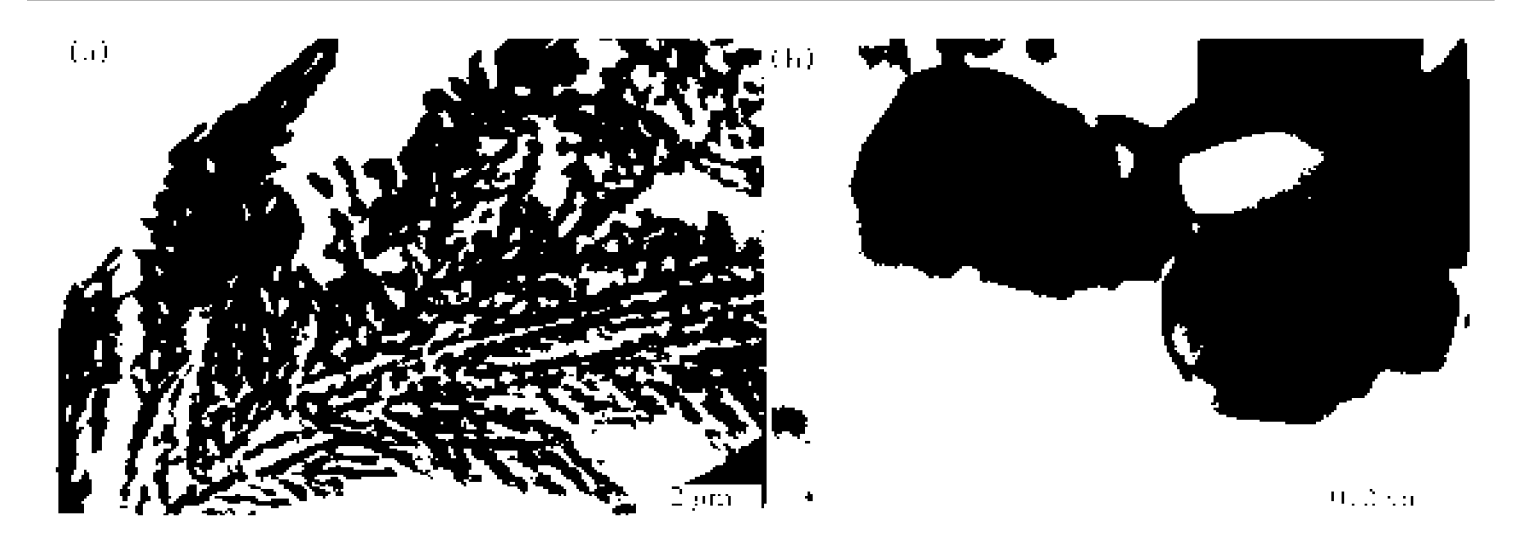


Fig. 4 TEM morphologies of quasicrystalline phase

(a) —Low-magnification morphology of dendritic element;
(b) —High-magnification morphology of polyhedron particles in dendrite element

axes and the dendrites are not perpendicular to each other, in fact, dense tassel-like shapes are observed, whose widths are about 8 µm. Considering the sizes of the quasicrystalline phase grains in Figs. 3(a) and (b), it can be concluded that the quasicrystalline phase grains consist of many tassel·like crystals or dendritic elements. The high magnification morphology in Fig. 4 (b) shows that each dendritic element is also composed of many polyhedron particles with a size of about 0.2 µm. Dubost et al [9] indicated that the growth morphology of the Al₆CuLi₃ icosahedral phase is dendritic polymers which are composed of triacontahedrons packed in the same directions, and that the triacontahedrons are the basic three dimensional Penrose units for ing[10, 11]. Similarly, the faceted dendrites in the Al₆₅Cu₂₀Fe₁₅ icosahedral phase are composed of dodecahedrons. However, the types and connecting modes of the polyhedrons found in this work needs further determination.

4 CONCLUSIONS

(1) The complex method of glass covering, salt denucleating and multiple superheating-cooling was applied to deal with the AFM n binary alloy, and a bulk AFM m (Si, B) quasicrystal-line alloy was produced through high undercooling. The Si and B elements were introduced by chemical reactions in the melting process.

- (2) The growth morphologies of the undercooled quasicrystalline phase are 5-fold or 3-fold symmetric faceted dendrites and have the same m3 5 point group symmetry as the quasicrystalline structure.
- (3) The quasicrystalline phase is composed of dendrite elements and the latters are composed of polyhedron particles.

REFERENCES

- Shechtman D, Blech I, Gratias D and Cahn J W. Phys Rev Lett, 1984, 53: 1951.
- Koskenmaki D C, Chen H S and Rao K V. Phys Rev b, 1986, 33(8): 5328.
- 3 Rajasekharan T, Gopalan R and Akhtar D. Scripta Metall, 1987, 21: 289.
- 4 Nissen H U, Wessicken R, Beeli C and Csanady A. Phil Mag B, 1988, 57: 587.
- 5 Zhang X and Kelton K F. Scripta Metall, 1992, 26: 393.
- 6 Chen Lifan and Chen Xichen. Journal of physics, (in Chinese), 1996, 45(1): 169.
- 7 Holland Moritz D, Herlach D M, Grushko B and Urban K. Mater Sci Eng, 1994, A181/A182: 766.
- 8 Guo Junqing and Li Qingchun. Progress in Materials Science, 1990, 4(5): 404.
- 9 Dubost B, Lang J M, Tanaka M, Sainfort P and Audier M. Nature, 1986, 324: 48.
- 10 Duneau M and Katz A. Phys Rev Lett, 1985, 54: 2688.
- 11 Elser V. Phys Rev, 1985, B32: 4892.

(Edited by Peng Chaoqun)